

# Photoassociation spectroscopy of ultracold metastable $^3\text{He}$ dimers

Daniel G. Cocks,<sup>‡a</sup> Gillian Peach,<sup>b</sup> and Ian B. Whittingham<sup>\*c</sup>

## Abstract

The bound states of the fermionic  $^3\text{He}(2\ ^3\text{S}_1)+^3\text{He}(2\ ^3\text{P}_j)$  system, where  $j = 0, 1, 2$ , are investigated using the recently available *ab initio* short-range  $^{1,3,5}\Sigma_{g,u}^+$  and  $^{1,3,5}\Pi_{g,u}$  potentials computed by Deguilhem *et al.* (*J. Phys. B: At. Mol. Opt. Phys.*, 2009, **42**, 015102). Single-channel and multichannel calculations have been undertaken in order to investigate the effects of Coriolis and non-adiabatic couplings. The possible experimental observability of the theoretical levels is assessed using criteria based upon the short-range character of each level and their coupling to metastable ground states. Purely long-range levels have been identified and 30 short-range levels near five asymptotes are suggested for experimental investigation.

## 1 Introduction

Photoassociation (PA) of ultracold atoms, in which two interacting ultracold atoms are resonantly excited by a laser to bound states of the associated molecule, is a widely used technique to study the dynamics of ultracold collisions in dilute quantum gases. Of particular interest is PA in metastable rare gases where novel experimental strategies based upon their large internal energy can be implemented.

Photoassociation of ultracold bosonic metastable  $^4\text{He}^*$  atoms,  $^4\text{He}(1s\ 2s\ ^3\text{S})$ , to excited rovibrational bound states that dissociate to the  $^4\text{He}(1s\ 2s\ ^3\text{S}) + ^4\text{He}(1s\ 2p\ ^3\text{P}_j)$  limits, where  $j = 0, 1, 2$ , has been observed by many groups. The observations include over 40 states lying within 14 GHz of the  $j = 2$  asymptote [1, 2, 3], six states within 0.6 GHz of the  $j = 1$  asymptote [3] and some purely long-range bound states within 1.43 GHz of the  $j = 0$  asymptote [4]. Theoretical analysis of the  $j = 0$  long-range states using single-channel [5] and multichannel [6] calculations based upon long-range Born-Oppenheimer potentials constructed from retarded resonance dipole and dispersion interactions gave excellent agreement with the measured binding energies. Analysis of the other states had to await the availability of short-range *ab initio*  $^{1,3,5}\Sigma_{g,u}^+$  and  $^{1,3,5}\Pi_{g,u}$  molecular potentials [7, 8] and was initially restricted to single-channel calculations [7, 8] which neglect non-adiabatic and Coriolis couplings. Very recently a detailed theoretical analysis of the entire  $^4\text{He}(1s\ 2s\ ^3\text{S}) + ^4\text{He}(1s\ 2p\ ^3\text{P}_j)$  system has been completed [9]. The role of these couplings was investigated using single-channel and multichannel calculations with the input potentials constructed from the short-range *ab initio* potentials of Deguilhem *et al.* [8] matched onto long-range retarded resonance dipole and dispersion po-

tentials. The multichannel calculations also permitted criteria to be established for the assignment of the theoretical levels to experimental observations based upon the short-range spin character of each level and their couplings to the metastable ground states. Excellent agreement was obtained for the numbers of observed levels and their binding energies after application of a 1% increase in the slope of the  $^5\Sigma_{g,u}^+$  and  $^5\Pi_{g,u}$  potentials near their inner classical turning point.

In contrast, PA of fermionic metastable  $^3\text{He}^*$  atoms,  $^3\text{He}(1s\ 2s\ ^3\text{S})$ , is relatively unexplored although they have been cooled and trapped [10] with comparable densities and temperatures to those of  $^4\text{He}^*$  atoms. The non-zero  $i = 1/2$  nuclear spin of  $^3\text{He}^*$  gives rise to hyperfine structure with splittings comparable to the fine structure splittings of  $^4\text{He}^*$  which has no nuclear spin. Consequently the patterns of energy levels is expected to be quite different for the fermionic and bosonic systems. A small number of long-range states in  $^3\text{He}^*$  has been predicted by Dickinson [11] but this was a single-channel calculation, thereby neglecting Coriolis and non-adiabatic couplings, using only long-range van der Waals and retarded resonance dipole interactions. The availability of the short-range potentials of Deguilhem *et al.* [8] now permits a detailed theoretical investigation of the fermionic  $^3\text{He}(1s\ 2s\ ^3\text{S}) + ^3\text{He}(1s\ 2p\ ^3\text{P}_j)$  system similar to that undertaken by Cocks *et al.* [9] for the bosonic  $^4\text{He}^*$  system.

In the absence of any observations of bound states in this excited  $^3\text{He}^*$  system, we present predictions as to which of our calculated bound states may be experimentally observable. We assume any experiment will use magnetic trapping of the  $^3\text{He}^*$  atoms, requiring all atoms to be in the fully stretched low-field seeking  $f = 3/2, m_f = 3/2$  magnetic substate of the metastable  $2s\ ^3\text{S}_1$  level in order to strongly suppress loss through Penning ionization. Consequently we assess the experimental observability of each excited level in terms of its coupling to this state. In addition, we consider the likelihood of ionization losses from these excited levels due to inelastic collisions in the short-range region.

Atomic units are used, with lengths in Bohr radii  $a_0 =$

<sup>a</sup> School of Engineering and Physical Sciences, James Cook University, Townsville 4811, Australia. E-mail: cocks@itp.uni-frankfurt.de

<sup>‡</sup> Present address: Institut für Theoretische Physik, Johann Wolfgang Goethe-Universität, 60438 Frankfurt/Main, Germany

<sup>b</sup> Department of Physics and Astronomy, University College London, London WC1E 6BT, UK. E-mail: g.peach@ucl.ac.uk

<sup>c</sup> School of Engineering and Physical Sciences, James Cook University, Townsville 4811, Australia. E-mail: ian.whittingham@jcu.edu.au

0.0529177209 nm and energies in Hartree  $E_h = \alpha^2 m_e c^2 = 27.211384$  eV.

## 2 Theory

### 2.1 Multichannel equations

The formalism for the excited  $^3\text{He}^*$  system requires modification of that presented in Cocks *et al.*[9] for the excited  $^4\text{He}^*$  system in order to include hyperfine structure.

The total Hamiltonian for a system of two interacting atoms  $i = 1, 2$  with reduced mass  $\mu$ , interatomic separation  $R$  and relative angular momentum  $\hat{\mathbf{L}}$ , which possess both fine structure and hyperfine structure is

$$\hat{H} = \hat{T} + \hat{H}_{\text{rot}} + \hat{H}_{\text{el}} + \hat{H}_{\text{fs}} + \hat{H}_{\text{hfs}} \quad (1)$$

where  $\hat{T}$  is the kinetic energy operator

$$\hat{T} = -\frac{\hbar^2}{2\mu R^2} \frac{\partial}{\partial R} \left( R^2 \frac{\partial}{\partial R} \right) \quad (2)$$

and  $\hat{H}_{\text{rot}}$  the rotational operator

$$\hat{H}_{\text{rot}} = \frac{\hat{L}^2}{2\mu R^2}. \quad (3)$$

The total electronic Hamiltonian is

$$\hat{H}_{\text{el}} = \hat{H}_1 + \hat{H}_2 + \hat{H}_{12}, \quad (4)$$

where the unperturbed atoms have Hamiltonians  $\hat{H}_i$  and their electrostatic interaction is specified by  $\hat{H}_{12}$ . The terms  $\hat{H}_{\text{fs}}$  and  $\hat{H}_{\text{hfs}}$  in equation (1) describe the fine structure and hyperfine structure respectively of the atoms.

The multichannel equations describing the interacting atoms are obtained from the eigenvalue equation

$$\hat{H}|\Psi\rangle = E|\Psi\rangle \quad (5)$$

for the total system by expanding the eigenvector in terms of an appropriate basis  $|\Phi_a\rangle = |\Phi_a(R, q)\rangle$  where  $a$  denotes the set of approximate quantum numbers describing the electronic-rotational states of the molecule and  $q$  denotes the interatomic polar coordinates  $(\theta, \varphi)$  and electronic coordinates  $(\mathbf{r}_1, \mathbf{r}_2)$ . Using the expansion

$$|\Psi\rangle = \sum_a \frac{1}{R} G_a(R) |\Phi_a\rangle \quad (6)$$

and forming the scalar product  $\langle \Phi_{a'} | \hat{H} | \Psi \rangle$  yields the multichannel equations

$$\sum_a \{ T_{a'a}^G(R) + [V_{a'a}(R) - E \delta_{a'a}] G_a(R) \} = 0, \quad (7)$$

where

$$T_{a'a}^G(R) = -\frac{\hbar^2}{2\mu} \langle \Phi_{a'} | \frac{\partial^2}{\partial R^2} G_a(R) | \Phi_a \rangle \quad (8)$$

and

$$V_{a'a}(R) = \langle \Phi_{a'} | [\hat{H}_{\text{rot}} + \hat{H}_{\text{el}} + \hat{H}_{\text{fs}} + \hat{H}_{\text{hfs}}] | \Phi_a \rangle. \quad (9)$$

We assume the  $R$ -dependence of the basis states is negligible so that the radial kinetic energy term is diagonalized:

$$T_{a'a}^G(R) = -\frac{\hbar^2}{2\mu} \frac{d^2 G_a}{dR^2} \delta_{aa'}. \quad (10)$$

### 2.2 Basis states

For two colliding atoms with orbital  $\hat{\mathbf{L}}_i$ , spin  $\hat{\mathbf{S}}_i$  and nuclear  $\hat{\mathbf{i}}_i$  angular momenta, the unsymmetrized body-fixed states in the coupling scheme

$$\hat{\mathbf{j}}_i = \hat{\mathbf{L}}_i + \hat{\mathbf{S}}_i, \quad \hat{\mathbf{f}}_i = \hat{\mathbf{j}}_i + \hat{\mathbf{i}}_i, \quad \hat{\mathbf{f}} = \hat{\mathbf{f}}_1 + \hat{\mathbf{f}}_2, \quad \hat{\mathbf{T}} = \hat{\mathbf{f}} + \hat{\mathbf{I}} \quad (11)$$

are (see appendix for details)

$$|(\gamma_1 j_1 i_1 f_1)_A, (\gamma_2 j_2 i_2 f_2)_B, f, \Omega_f, T, m_T\rangle \quad (12)$$

where  $\gamma_i \equiv \{\bar{\gamma}_i, L_i, S_i\}$ ,  $\bar{\gamma}_i$  representing any other relevant quantum numbers, and  $(A, B)$  labels the two nuclei. The projections of an angular momentum  $\hat{\mathbf{J}}$  onto the space-fixed  $Oz$  and inter-molecular axis  $OZ$  with orientation  $(\theta, \varphi)$  relative to the space-fixed frame will be denoted  $m_J$  and  $\Omega_J$  respectively.

In order to construct states symmetrized with respect to the total parity  $\hat{P}_T$  we note that  $\hat{P}_T = \hat{P}_L \hat{P}_S \hat{P}_i \hat{X}_N$  where  $\hat{P}_L, \hat{P}_S, \hat{P}_i$  are the inversion operators on the orbital, electronic spin and nuclear spin states associated respectively with

$$\hat{\mathbf{L}} = \hat{\mathbf{L}}_1 + \hat{\mathbf{L}}_2, \quad \hat{\mathbf{S}} = \hat{\mathbf{S}}_1 + \hat{\mathbf{S}}_2, \quad \hat{\mathbf{i}} = \hat{\mathbf{i}}_1 + \hat{\mathbf{i}}_2 \quad (13)$$

and  $\hat{X}_N$  permutes the nuclei labels. The states of total parity are then (see appendix)

$$\begin{aligned} & |(\alpha_1)_A, (\alpha_2)_B, f, \phi, T, m_T; P_T\rangle = \\ & N_{P_T} [ |(\alpha_1)_A, (\alpha_2)_B, f, \phi, T, m_T\rangle \\ & + P_T P_1 P_2 (-1)^{f-T} |(\alpha_1)_A, (\alpha_2)_B, f, -\phi, T, m_T\rangle ] \end{aligned} \quad (14)$$

where  $\alpha_i \equiv \{j_i, l_i, i_i, f_i\}$ ,  $P_i = (-1)^{L_i}$  is the parity of the atomic state  $|L_i, m_{L_i}\rangle$  and  $\phi = |\Omega_f| = |\Omega_T|$ . The normalization constant is  $N_{P_T} = 1/\sqrt{2(1 + \delta_{\phi,0})}$ . For  $\phi = 0$  equation (14) gives the selection rule  $P_T P_1 P_2 (-1)^{f-T} = 1$ .

The states symmetrized with respect to  $\hat{X}_N$  are (see appendix)

$$\begin{aligned} & |\alpha_1, \alpha_2, f, \phi, T, m_T; P_T, X_N\rangle = \\ & N_{X_N} [ |(\alpha_1)_A, (\alpha_2)_B, f, \phi, T, m_T; P_T\rangle \\ & + \varepsilon_N |(\alpha_2)_A, (\alpha_1)_B, f, \phi, T, m_T; P_T\rangle ] \end{aligned} \quad (15)$$

where  $P_N = (-1)^{2i_1}$  indicates bosonic or fermionic nuclei (where  $i_1 = i_2$  is assumed),  $N_i$  is the number of electrons on atom  $i$ , the normalization constant  $N_{X_N}$  is  $1/\sqrt{2(1 + \delta_{\alpha_1, \alpha_2})}$  and the phase factor is

$$\varepsilon_N = P_N P_T P_1 P_2 (-1)^{f_1 + f_2 - f + N_1 N_2}. \quad (16)$$

For  $\alpha_1 = \alpha_2$ , equation (15) gives the selection rule  $P_N P_T P_1 P_2 (-1)^{f_1 + f_2 - f + N_1 N_2} = 1$ .

It is convenient to introduce the simplified notation

$$|\alpha_1, \alpha_2, \phi\rangle = N_{X_N} [ |(\alpha_1)_A, (\alpha_2)_B, f, \phi, T, m_T\rangle + \varepsilon_N |(\alpha_2)_A, (\alpha_1)_B, f, \phi, T, m_T\rangle ] \quad (17)$$

so that the states (15) can then be written

$$|\alpha_1, \alpha_2, f, \phi, T, m_T; P_T, X_N\rangle = N_{P_T} [ |\alpha_1, \alpha_2, \phi\rangle + P_T P_1 P_2 (-1)^{f-T} |\alpha_2, \alpha_1, -\phi\rangle ]. \quad (18)$$

The eigenstates of  $\hat{H}_{\text{el}}$  are the body-fixed states arising from the couplings  $\hat{\mathbf{L}} = \hat{\mathbf{L}}_1 + \hat{\mathbf{L}}_2$ ,  $\hat{\mathbf{S}} = \hat{\mathbf{S}}_1 + \hat{\mathbf{S}}_2$  and must be symmetric under the action of  $\hat{P}_L \hat{P}_S$ :

$$|\gamma_1 \gamma_2, LS\Omega_L \Omega_S; w\rangle = N_w [ |(\gamma_1)_A (\gamma_2)_B, LS\Omega_L \Omega_S\rangle + \varepsilon_w |(\gamma_2)_A (\gamma_1)_B, LS\Omega_L \Omega_S\rangle ] \quad (19)$$

where  $N_w = 1/\sqrt{2(1 + \delta_{\gamma_1, \gamma_2})}$ ,  $w = 0(1)$  for *gerade* (*ungerade*) symmetry and

$$\varepsilon_w = (-1)^{w+L_1+L_2+S_1+S_2-S+N_1 N_2} P_1 P_2. \quad (20)$$

The relationship between the two bases (17) and (19) is obtained using (see appendix)

$$|\alpha_1, \alpha_2, \phi\rangle = N_{X_N} N_w |T, m_T, \phi\rangle \sum_{ij\Omega_i\Omega_j} \sum_{LS\Omega_L\Omega_S} F_{ji\Omega_j\Omega_i}^{f_1 f_2 f \phi} F_{LS\Omega_L\Omega_S}^{j_1 j_2 j \Omega_j} \times [ (|g\rangle + |u\rangle) + \varepsilon (|g\rangle - |u\rangle) ] |(\alpha_1)_A (\alpha_2)_B, i\Omega_i\rangle \quad (21)$$

where the coupling coefficients  $F_{ji\Omega_j\Omega_i}^{f_1 f_2 f \phi}$  and  $F_{LS\Omega_L\Omega_S}^{j_1 j_2 j \Omega_j}$  are given in the appendix (the quantum numbers  $(L_i, S_i, i_i)$  have been suppressed) and we have introduced the notation

$$|g\rangle = |\gamma_1 \gamma_2, LS\Omega_L \Omega_S; g\rangle, \quad |u\rangle = |\gamma_1 \gamma_2, LS\Omega_L \Omega_S; u\rangle \quad (22)$$

for the eigenstates of *gerade* and *ungerade* symmetry. The rotational states are

$$|T, m_T, \phi\rangle = \sqrt{\frac{2T+1}{4\pi}} D_{m_T, \phi}^{T*}(\varphi, \theta, 0), \quad (23)$$

where  $D_{m_T, \phi}^{T*}(\varphi, \theta, 0)$  is the Wigner rotation matrix, and the phase factor is

$$\varepsilon = P_N P_T (-1)^{2i_1 + 2f + i - 2S}. \quad (24)$$

For the  ${}^3\text{He}(1s\ 2s\ {}^3\text{S}) + {}^3\text{He}(1s\ 2p\ {}^3\text{P}_j)$  system,  $\alpha_1 = (\tilde{\gamma}_1, 0, 1, 1, 1/2, f_1)$  and  $\alpha_2 = (\tilde{\gamma}_2, 1, 1, j_2, 1/2, f_2)$  and (21) reduces to

$$\begin{aligned} |\alpha_1, \alpha_2, \phi\rangle = & |T, m_T, \phi\rangle \sum_{ij\Omega_i\Omega_j} \sum_{S\Omega_L\Omega_S} (-1)^{1-j_2} [ijf_1 f_2 S j_2]^{1/2} \\ & \times C_{\Omega_j \Omega_i \phi}^{jif} C_{\Omega_L \Omega_S \Omega_j}^{1Sj} \begin{Bmatrix} 1 & j_2 & j \\ 1/2 & 1/2 & i \\ f_1 & f_2 & f \end{Bmatrix} \begin{Bmatrix} 1 & 1 & j_2 \\ 1 & j & S \end{Bmatrix} \\ & \times \frac{1}{2} [ (|g\rangle + |u\rangle) + P_T (-1)^i (|g\rangle - |u\rangle) ] \\ & \times |(\alpha_1)_A (\alpha_2)_B, i\Omega_i\rangle \end{aligned} \quad (25)$$

where  $C_{m_1 m_2 m}^{j_1 j_2 j}$  is a Clebsch-Gordan coefficient,  $\begin{Bmatrix} a & b & c \\ d & e & f \end{Bmatrix}$  and  $\begin{Bmatrix} a & b & c \\ d & e & f \\ g & h & i \end{Bmatrix}$  are Wigner 6- $j$  and 9- $j$  symbols respectively and  $[ab\dots] = (2a+1) \times (2b+1) \times \dots$

### 2.3 Matrix elements

The multichannel equations (7) require the matrix elements of  $\hat{H}_{\text{rot}}$ ,  $\hat{H}_{\text{el}}$ ,  $\hat{H}_{\text{fs}}$  and  $\hat{H}_{\text{hfs}}$  in the basis (17). Using the notation  $|a\rangle = |\Phi_a(R, q)\rangle$  where  $a \equiv \{\alpha_1, \alpha_2, f, \phi, T, m_T, P_T, X_N\}$  then the rotation terms are

$$\begin{aligned} \langle a' | \hat{I}^2 | a \rangle = & \hbar^2 \delta_{\rho, \rho'} \{ [T(T+1) + f(f+1) - 2\phi^2] \delta_{\phi', \phi} \\ & - K_{Tf\phi}^- \delta_{\phi', \phi-1} - K_{Tf\phi}^+ \delta_{\phi', \phi+1} \}, \end{aligned} \quad (26)$$

where the Coriolis coupling terms are

$$\begin{aligned} K_{Tf\phi}^\pm = & [T(T+1) - \phi(\phi \pm 1)]^{\frac{1}{2}} \\ & \times [f(f+1) - \phi(\phi \pm 1)]^{\frac{1}{2}} \end{aligned} \quad (27)$$

and  $\rho$  denotes the set of quantum numbers  $\{\alpha_1, \alpha_2, f, T, m_T, P_T\}$ .

The electronic matrix elements can be expressed in terms of the Born-Oppenheimer (BO) molecular potentials  ${}^{2S+1}\Lambda_w^\sigma(R)$ , where  $\Lambda = |\Omega_L|$  and  $\sigma$  is the symmetry of the electronic wave function with respect to reflection through a plane containing the internuclear axis, using

$$\hat{H}_{\text{el}} |\gamma_1 \gamma_2, LS\Omega_L \Omega_S; w\rangle = [{}^{2S+1}\Lambda_w^\sigma(R) + E_{\Lambda S}^\infty] |\gamma_1 \gamma_2, LS\Omega_L \Omega_S; w\rangle \quad (28)$$

where  $E_{\Lambda S}^\infty$  is the asymptotic energy of the state. The result is (see appendix)

$$\begin{aligned} \langle a' | \hat{H}_{\text{el}} | a \rangle = & \delta_{\eta, \eta'} \sum_{j' i S \Omega_L \Omega_i} \sum (-1)^{j_2 + j'_2 + j + j'} [f_1 f'_1 f_2 f'_2 j_2 j'_2 f f']^{1/2} \end{aligned}$$

$$\begin{aligned}
& \times [S_i j j'] \begin{pmatrix} j & i & f \\ \Omega_j & \Omega_i & -\phi \end{pmatrix} \begin{pmatrix} j' & i & f' \\ \Omega_j & \Omega_i & -\phi \end{pmatrix} \\
& \times \begin{pmatrix} 1 & S & j \\ \Omega_L & \Omega_S & \Omega_i - \phi \end{pmatrix} \begin{pmatrix} 1 & S & j' \\ \Omega_L & \Omega_S & \Omega_i - \phi \end{pmatrix} \\
& \times \begin{Bmatrix} 1 & j_2 & j \\ 1/2 & 1/2 & i \end{Bmatrix} \begin{Bmatrix} 1 & j_2 & j \\ 1/2 & 1/2 & i \end{Bmatrix} \\
& \times \begin{Bmatrix} 1 & 1 & j_2 \\ f_1 & f_2 & f \end{Bmatrix} \begin{Bmatrix} 1 & 1 & j_2 \\ f'_1 & f'_2 & f \end{Bmatrix} \\
& \times \begin{Bmatrix} 1 & 1 & j_2 \\ 1 & j & S \end{Bmatrix} \begin{Bmatrix} 1 & 1 & j'_2 \\ 1 & j' & S \end{Bmatrix} \\
& \times \frac{1}{2} \{ 2^{2S+1} \Lambda_g^+(R) + 2^{2S+1} \Lambda_u^+(R) + 2E_{\Lambda S}^\infty \\
& + P_T (-1)^i [2^{2S+1} \Lambda_g^+(R) - 2^{2S+1} \Lambda_u^+(R)] \} \quad (29)
\end{aligned}$$

where  $\begin{pmatrix} a & b & c \\ d & e & f \end{pmatrix}$  is a Wigner  $3-j$  coefficient,  $\Omega_S = \phi - \Omega_i - \Omega_L$  and  $\eta$  denotes the set of quantum numbers  $\{\gamma_1, \gamma_2, \phi, T, m_T, P_T\}$ . This equation differs from that given by Dickinson [11] by an overall phase factor  $(-1)^{1-i-\Omega_i}$  and the phase of the  $\Lambda_g - \Lambda_u$  term.

The matrix elements of the fine structure and hyperfine structure are best expressed in the basis

$$|\alpha_i, m_{f_i}\rangle = \sum_{m_{j_i}, m_i, m_L, m_{S_i}} C_{m_{j_i}, m_i, m_{f_i}}^{j_i, i, f_i} C_{m_L, m_{S_i}, m_{j_i}}^{L_i, S_i, j_i} |\gamma, m_L, m_{S_i}\rangle |i, m_i\rangle. \quad (30)$$

For convenience we omit the label  $m_{f_i}$  from these states as the matrix elements of  $\hat{H}_{fs}$  and  $\hat{H}_{hfs}$  are independent of  $m_{f_i}$  due to rotational invariance. We assume that the fine structure is independent of  $R$  and exclude couplings to the singlet atomic state  $S_i = 0$  so that its contribution is

$$\langle \alpha'_i | \hat{H}_{fs} | \alpha_i \rangle = \delta_{\alpha_i, \alpha'_i} \Delta E_{\gamma_i j_i}^{fs}. \quad (31)$$

The fine structure splitting  $\Delta E_{\gamma_1 j_1}^{fs}$  for the  $2s^3S_1$  level vanishes and the splittings  $\Delta E_{\gamma_2 j_2}^{fs}$  for the  $2p^3P_0$  and  $2p^3P_1$  states relative to the  $2p^3P_2$  level are 31.9088 GHz and 2.2922 GHz respectively [13].

Matrix elements for the hyperfine structure have been obtained by Hinds *et al.* [12] and Wu and Drake [13]. We choose to use the expression of Wu and Drake but exclude couplings to the  $S_i = 0$  atomic states. The matrix elements are therefore

$$\begin{aligned}
& \langle \alpha'_i | \hat{H}_{hfs} | \alpha_i \rangle = \\
& \delta_{\gamma_i, \gamma'_i} W_{j_i j'_i}^{i, f_i} \left[ C_{S_i} \sqrt{6} (-1)^{L_i + j'_i} X_{S_i} \begin{Bmatrix} S'_i & j'_i & L_i \\ j_i & S_i & 1 \end{Bmatrix} \right. \\
& - D_{S_i} (-1)^{j_i + S_i + M} \begin{Bmatrix} L_i & j'_i & S_i \\ j_i & L_i & 1 \end{Bmatrix} \begin{pmatrix} L_i & 1 & L_i \\ -M & 0 & M \end{pmatrix}^{-1} \\
& + E_{S_i} \frac{12}{\sqrt{5}} (-1)^{S_i - L_i + M} X_{S_i} \\
& \left. \times \begin{Bmatrix} L_i & L_i & 2 \\ S_i & S_i & 1 \\ j'_i & j_i & 1 \end{Bmatrix} \begin{pmatrix} L_i & 2 & L_i \\ -M & 0 & M \end{pmatrix}^{-1} \right] \quad (32)
\end{aligned}$$

where these expressions are to be evaluated with  $M = L_i$ ,

$$W_{j_i j'_i}^{i, f_i} = (-1)^{j_i + i + f_i} i_i [j_i j'_i]^{1/2} \begin{Bmatrix} f_i & i_i & j'_i \\ 1 & j_i & i_i \end{Bmatrix} \begin{pmatrix} i_i & 1 & i_i \\ -i_i & 0 & i_i \end{pmatrix}^{-1} \quad (33)$$

and

$$X_{S_i} = -(2S_i + 1) \begin{Bmatrix} 1/2 & S_i & 1/2 \\ S_i & 1/2 & 1 \end{Bmatrix}. \quad (34)$$

The hyperfine structure parameters (in MHz) are [13]

$$C_1 = -4283.85, \quad D_1 = -28.145, \quad E_1 = 7.126. \quad (35)$$

The inclusion of hyperfine structure using (32) couples states with the same  $L_i, S_i$  and  $f_i$  but different  $j_i$  and for the He  $2p^3P$  manifold the states  $(j, f) = (0, 1/2)$  and  $(1, 1/2)$  are significantly coupled as are the pair  $(j, f) = (1, 3/2)$  and  $(2, 3/2)$ . The eigenvalues of  $\hat{H}_{fs} + \hat{H}_{hfs}$  give the following energies for the hyperfine levels expressed relative to the state  $j = 2, f = 5/2$ : 0, 1780.851, 6292.906, 6961.065 and 34385.941 MHz. The eigenvectors give the mixing coefficients which are then used to modify the purely algebraic transformation to the hyperfine case given by equation (30). For the hyperfine structure of the  $2s^3S$  level we adopt the splitting of 6739.701177 MHz as measured by Zhao *et al.* [14]. This data then gives the ten asymptotic energies  $E_N^\infty$  of the separated pairs of atoms as 0, 1780.851, 6292.906, 6739.701, 6961.065, 8520.552, 13032.607, 13700.766, 34385.941 and 41125.642 MHz.

We assume that the fine- and hyperfine- structure of the individual atoms is not affected by their participation within the dimer, so that we may write

$$\begin{aligned}
& \langle a' | \hat{H}_{fs} + \hat{H}_{hfs} | a \rangle = \\
& \delta_{a'a} (\Delta E_{\gamma_1 j_1}^{fs} + \Delta E_{\gamma_2 j_2}^{fs}) + \delta_{\sigma', \sigma} (\langle \alpha'_1 | \hat{H}_{hfs} | \alpha_1 \rangle \delta_{\alpha'_2, \alpha_2} \\
& + \langle \alpha'_2 | \hat{H}_{hfs} | \alpha_2 \rangle \delta_{\alpha'_1, \alpha_1}) \quad (36)
\end{aligned}$$

where  $\sigma$  denotes the set of quantum numbers  $\{f, \phi, T, m_T, P_T\}$ .

The total matrix element  $V_{a'a}(R)$  is therefore diagonal in  $\{T, P_T\}$  and independent of  $m_T$ . The  $m_T$ -degenerate discrete multichannel eigenenergies of (7) are then  $E_{T, P_T, \nu}$  where  $\nu$  labels the rovibrational levels.

## 2.4 Single-channel approximation

The single-channel approximation involves the neglect of the Coriolis couplings in (26) and non-adiabatic couplings in the kinetic energy term. At each value of  $R$  the single-channel potential is formed by diagonalizing the matrix:

$$V_{aa}^\phi = \langle a' | \hat{H}_{el} | a \rangle + \langle a' | (\hat{H}_{fs} + \hat{H}_{hfs}) | a \rangle + \frac{\langle a' | \hat{I}^2 | a \rangle \phi}{2\mu R^2}, \quad (37)$$

where  $\langle a' | \hat{I}^2 | a \rangle_\phi$  is the part of (26) diagonal in  $\phi$ . The corresponding  $R$ -dependent eigenvectors are

$$|n\rangle = \sum_a C_{an}(R) |a\rangle \quad (38)$$

and the adiabatic potential is given by  $V_n^{\text{adi}}(R) = \sum_{a'a} C_{a'n}^{-1} V_{a'a}^\phi C_{an}$ . Each channel  $|n\rangle$  can be labelled with the notation  $\{\phi, T, m_T, P_T\}$ .

The adiabatic eigenvalue equation for the rovibrational eigenstates  $|\psi_{n,v}\rangle = R^{-1} G_{n,v}(R) |i\rangle$ , where  $n = \{\phi, T, m_T, P_T\}$ , is then obtained by neglecting the off-diagonal (non-adiabatic) couplings between different single-channel states in the kinetic energy term so that

$$\langle n' | \hat{T} \frac{1}{R} G_{n,v}(R) | n \rangle = -\frac{\hbar^2}{2\mu R} \frac{d^2 G_{n,v}}{dR^2} \delta_{n,n'}. \quad (39)$$

The radial eigenvalue equation for the rovibrational states is then

$$\left[ -\frac{\hbar^2}{2\mu} \frac{d^2}{dR^2} + V_n^{\text{adi}}(R) - E_{n,v} \right] G_{n,v}(R) = 0. \quad (40)$$

## 2.5 Input potentials

The required Born-Oppenheimer potentials  $^{1,3,5}\Sigma_{g,u}^+$  and  $^{1,3,5}\Pi_{g,u}$  were constructed as in Cocks *et al.*[9] by matching the *ab initio* short-range potentials of Deguilhem *et al.*[8] onto the long-range dipole-dipole plus dispersion potentials

$$V_\Lambda^{\text{long}}(R) = -f_{3\Lambda}(R/\tilde{\lambda}) C_{3\Lambda}/R^3 - C_{6\Lambda}/R^6 - C_{8\Lambda}^\pm/R^8 - C_{9\Lambda}/R^9 - C_{10\Lambda}/R^{10}, \quad (41)$$

where  $f_{3\Lambda}$  is an  $R$ - and  $\Lambda$ -dependent retardation correction [16],  $\tilde{\lambda} = \lambda/(2\pi) = 3258.12a_0$  where  $\lambda$  is the wavelength for the  $2s^3S-2p^3P$  transition and the parameters  $C_{n\Lambda}$  were taken from Zhang *et al.*[15].

Motivated by our study of the  $^4\text{He}^*$  system [9], we choose to vary the quintet potentials through a modification of the slope of the potential at the inner classical turning point by introducing a multiplicative factor  $c$  through the smoothing function

$$V'(R) = \begin{cases} V(R)(1+2c) & R \leq R_1 \\ V(R)[1+c(1+\cos a(R-R_1))] & R_1 < R \leq R_2 \\ V(R) & R > R_2 \end{cases}, \quad (42)$$

where  $R_1 = 5a_0$ ,  $R_2 = 10a_0$  and  $a = \pi/(R_2 - R_1)$ . The value  $c = 0.005$  represents a 1% variation which is quickly turned on through the region  $5 < R < 10a_0$ . Its effect is to deepen the minimum of the attractive  $^5\Pi_g$  potential at  $R = 5.387a_0$  by 0.985% and move it to a smaller interatomic separation by  $0.003a_0$ . The depth of the minimum in the  $^5\Sigma_u^+$  potential at  $R = 6.268a_0$  is increased by 0.851% and is moved towards a

smaller separation by  $0.010a_0$ . The other quintet potentials  $^5\Sigma_g^+$  and  $^5\Pi_u$  are not significantly affected as they are repulsive.

## 3 Results

### 3.1 Calculations

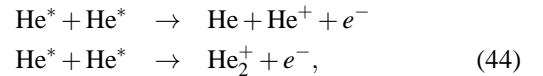
The coupled-channel equations (7) and the single-channel equation (40) are of the form

$$\left[ \mathbf{I} \frac{d^2}{dR^2} + \mathbf{Q}(R) \right] \mathbf{G}(R) = 0, \quad (43)$$

where for the case of coupled-channels,  $\mathbf{G}$  is the matrix of solutions with the second subscript labelling the linearly independent solutions. These equations were solved using the renormalized Numerov method [17] with the eigenvalues of the purely bound states determined by counting the nodes of the determinant  $|\mathbf{G}(R)|$  and the energies of resonances lying within open channels by using a search procedure based on Cauchy's argument principle applied to the determinant  $D(E) = |\mathbf{R}_m - \hat{\mathbf{R}}_{m+1}^{-1}|$  where  $\mathbf{R}_m$  and  $\hat{\mathbf{R}}_{m+1}$  are ratio matrices for the outward and inward integrations respectively of the renormalized Numerov method. Further numerical details are given in Cocks *et al.*[9].

### 3.2 Observability Criteria

In order to predict the likelihood that calculated bound levels may appear in future experiments, several properties are determined for each bound level or resonance that we isolate. The simplest of these is the proportion  $P_{\text{short}}$  of wave function present at close interatomic distances, defined as  $R < 20a_0$  and henceforth referred to as the short-range region. This property is extremely useful in classifying results since ionization losses, which arise from the inelastic collisions



only occur in the short-range region. As has been observed in bosonic metastable helium, there exist indications of purely long-range states in the fermionic dimers investigated here, and we define these by  $P_{\text{short}} < 10^{-10}$ .

If the level extends into the short-range region then an indication of its propensity for ionization is obtained from the proportion  $P_{\text{str}}$  of wave function that is in the spin-stretched  $S = 2, i = 1$  configuration:

$$P_{\text{str}} = \frac{\sum_{a,b} \delta_{S,2} \delta_{i,1} P_{ab}}{\sum_{a,b} P_{ab}} \quad (45)$$

where

$$P_{ab} = \langle a|b \rangle \int_0^{20a_0} G_a(R) dR \quad (46)$$

and  $|b \rangle \equiv |\gamma_1 \gamma_2, LS\Omega_L \Omega_S w \rangle |(i_1)_A (i_2)_B, i\Omega_i \rangle$  is the complete LS basis state. The transformation between the bases used here can be found from equation (21). As in the  $^4\text{He}^*$  case, the ionization rate of the dimers is significantly reduced in the spin-stretched state [18]. Hence, a large proportion of wave function in the spin-stretched state is essential for the level to have a lifetime long enough to be observed in experiment.

Finally, for a resonance to be observed in PA experiments, it must be strongly coupled by a laser pulse to the metastable manifold  $^3\text{He}(1s 2s \ ^3S_1) + ^3\text{He}(1s 2s \ ^3S_1)$ . For radiation of circular polarization  $\varepsilon_\lambda$  the coupling between a metastable dimer state and the excited dimer state is due to the interaction  $\hat{H}_{\text{int}} \sim \varepsilon_\lambda \cdot \hat{\mathbf{d}}$  where  $\hat{\mathbf{d}}$  is the molecular dipole moment and is given by

$$\begin{aligned} \langle e' | \hat{H}_{\text{int}} | g \rangle = & \\ & -i(-1)^\lambda \sqrt{\frac{I}{\varepsilon_0 c}} \sqrt{\frac{2T+1}{2T'+1}} C_{m_T \lambda m_T}^{T 1 T'} C_{\phi \beta \phi'}^{T 1 T'} \frac{N_{X_N}}{2} d_{\text{at}} \\ & \times \sum_{iSj'} \sum_{\Omega_i \Omega_j \Omega_j'} (-1)^{1-j'_2} [iS] [j' f'_1 f'_2 j'_2 f_1 f_2]^{1/2} \\ & \times C_{\Omega_j' \Omega_i \Omega_j'}^{j' i f'} C_{\beta \Omega_S \Omega_j'}^{1 S j'} C_{\Omega_S \Omega_i \phi}^{S i f} \begin{Bmatrix} 1 & 1 & j'_2 \\ 1 & j' & S \end{Bmatrix} \\ & \times \begin{Bmatrix} 1 & j'_2 & j' \\ 1/2 & 1/2 & i \end{Bmatrix} \begin{Bmatrix} 1 & 1 & S \\ 1/2 & 1/2 & i \end{Bmatrix} \begin{Bmatrix} f_1 & f_2 & f \end{Bmatrix} \quad (47) \end{aligned}$$

where  $|g \rangle$  and  $|e \rangle$  are basis states corresponding to the  $^3\text{He}(1s 2s \ ^3S_1) + ^3\text{He}(1s 2s \ ^3S_1)$  and  $^3\text{He}(1s 2s \ ^3S_1) + ^3\text{He}(1s 2s \ ^3P_j)$  manifolds respectively,  $\beta = \phi' - \phi$  and only those matrix elements with  $P_T' P_T = -1$  and  $|\beta| \leq 1$  are non-zero. The atomic dipole moment is given by  $d_{\text{at}}$ . Note that the metastable spin-stretched state has  $P_T = +1$  symmetry and can therefore only be coupled to excited dimers of  $P_T = -1$  symmetry.

Finally, we define the quantities

$$\mathcal{A}_{\text{str}} = \frac{1}{N_{g'}} \sum_{g'a} \langle a | \hat{H}_{\text{int}} | g' \rangle \int G_{g'}(R) G_{a,v}(R) dR, \quad (48)$$

where  $g'$  enumerates all of the  $N_{g'}$  spin-stretched metastable dimer states, and

$$\mathcal{A}_{\text{full}} = \frac{1}{N_g} \sum_{g'a} \langle a | \hat{H}_{\text{int}} | g \rangle \int G_g(R) G_{a,v}(R) dR \quad (49)$$

where  $g$  enumerates all of the  $N_g$  metastable dimer states. The true metastable radial wave functions  $G_g(R)$  depend upon temperature, but in order to extract a single parameter for the observability criteria, we take  $G_g(R) = 1$  as was done in the  $^4\text{He}^*$

case. This is valid up to a constant factor when the metastable wave functions do not change significantly with temperature. Although we focus on predicting resonances observable from experiments prepared with spin-stretched states in this paper, due to the overwhelming benefits from reduced trap loss, whenever it is convenient we also include the likelihood for couplings from other metastable states. Spin-stretched experiments are best described by the criterion  $\mathcal{A}_{\text{str}}$ , whereas experiments that do not polarize the metastable gas are best described by the criterion  $\mathcal{A}_{\text{full}}$ .

### 3.3 Single-channel

The binding energies of long-range states obtained using a single-channel calculation are listed in Tables 1 and 2. The single-channel levels are labelled in terms of  $\{T, \phi^{P_T}\}$ .

Levels which are strongly coupled to the spin-stretched metastable dimer states are indicated by a superscript 1. In the absence of existing experimental data, we use the same criterion to that obtained for the  $^4\text{He}^*$  case, that is  $\mathcal{A}_{\text{str}} > 0.9 E_h$ . As these are long-range levels, there is no possibility of ionization and we can ignore the  $P_{\text{str}}$  condition. Furthermore, levels that are strongly coupled to the unpolarized metastable dimer states are indicated by a superscript 2, where the criterion is  $\mathcal{A}_{\text{full}} > 0.9 E_h$ .

Of the 159 long-range levels found, 15 have a strong spin-stretched coupling, and 69 have a strong unpolarized coupling. In addition, there are 151 levels that possess some short-range character, and also satisfy the observability criteria. Some of these are very strongly coupled to the spin-stretched metastable state. However, we do not observe these levels once non-adiabatic and Coriolis couplings are turned on and so conclude that these levels are unlikely to be observed in experiment.

### 3.4 Multichannel

With all couplings included in the calculation, only those levels beneath the lowest asymptote are true bound states. In contrast to the situation in  $^4\text{He}^*$ , most of the levels lie above the lowest asymptote and, due to couplings to open channels, these higher lying levels almost always acquire a finite lifetime due to predissociation. These resonances possess complex energies, where the imaginary component represents the resonance width, and are more difficult to isolate. As our search routine based on Cauchy's argument principle requires many solutions of the differential equations (7), we restrict the predissociation width to be less than 100 MHz and only search within 2 GHz of the asymptotic energies that result from diagonalization of the hyperfine structure. Additionally, we match only at two points, 100 and 300  $a_0$ , which may exclude a few levels from our search, although it can be argued on the ba-

**Table 1** Single-channel rovibrational binding energies, in units of MHz, of long-range  $0^\pm$  and  $1^\pm$  states in  ${}^3\text{He}(2\ {}^3\text{S}_1)+{}^3\text{He}(2\ {}^3\text{P}_j)$ . Energies given are relative to the energy of the specified asymptote. The superscripts 1 and 2 indicate those states which satisfy the strong coupling conditions  $\mathcal{A}_{\text{str}} > 0.9 E_h$  and  $\mathcal{A}_{\text{full}} > 0.9 E_h$  respectively.

Symmetry	State No.	Asymp. No.	$\nu/T$	0	1	2	3	4
$0^+$	5	3	0	904.113		823.629		639.703
			1	183.326		127.625		9.53314
	6	4	0	347.642		262.537 <sup>2</sup>		75.7138 <sup>2</sup>
			1	10.8473				
	10	6	0		1422.19		1278.29	
			1		467.747		366.810	
			2		62.6480		11.3740	
	11	8	16		52.8477 <sup>2</sup>		27.0296	
			17		11.6235			
	12	9	0		202.645 <sup>2</sup>		52.0862 <sup>2</sup>	
			1		13.4273			
	$0^-$	7	5	0	6.10337			
10		7	0	374.065	1425.59	296.578 <sup>2</sup>	1271.97 <sup>2</sup>	126.120 <sup>2</sup>
			1	40.4103	579.160	8.45110	449.478	
			2		173.330		99.6096	
			3		37.9230			
11		8	16		940.315 <sup>2</sup>		815.427 <sup>2</sup>	
			17		503.466 <sup>2</sup>		417.433	
			18		227.478 <sup>2</sup>		172.257	
			19		86.2920 <sup>2</sup>		55.4097	
			20		24.2101 <sup>2</sup>		9.30074	
12		9	16		500.709 <sup>2</sup>		319.184 <sup>2</sup>	
			17		131.414		47.6889	
			18		19.7607			
13		10	0		741.860 <sup>2</sup>		547.258 <sup>2</sup>	
			1		233.251		130.685 <sup>2</sup>	
			2		51.1549		11.7006	
			3		5.72522			
$1^+$		17	7	0		1269.28	1214.50 <sup>2</sup>	1132.90
	1				405.296	366.915	310.695 <sup>2</sup>	238.337
	2				74.8580	55.8199	29.9220	1.87478
	3				6.48198			
	18	8	0		918.791 <sup>2</sup>	869.335 <sup>2</sup>	796.261 <sup>2</sup>	701.007
			1		432.677 <sup>2</sup>	401.217	355.166 <sup>2</sup>	295.970
			2		180.375 <sup>2</sup>	160.938	133.043 <sup>2</sup>	98.3456
			3		62.5650 <sup>2</sup>	52.0562	37.1800 <sup>2</sup>	20.8902
			4		15.6929	10.8815		
	20	9	0		438.234 <sup>2</sup>	366.110 <sup>2</sup>	264.239 <sup>2</sup>	141.524 <sup>2</sup>
			1		106.356	73.1955 <sup>2</sup>	31.0864	
			2		14.2935	5.04058		
22	10	5		91.4710 <sup>2</sup>	58.1199 <sup>2</sup>	16.2073 <sup>2</sup>		
		6		8.96832	1.27172			
$1^-$	11	4	0		526.589 <sup>1</sup>	465.051 <sup>1,2</sup>	374.249 <sup>1,2</sup>	256.239
			1		31.3952	6.28362 <sup>1,2</sup>		
	12	5	0		30.9200 <sup>1,2</sup>			
17	7	0		342.560 <sup>2</sup>	290.731 <sup>1,2</sup>	214.234 <sup>1,2</sup>	114.816 <sup>2</sup>	

**Table 2** Single-channel rovibrational binding energies, in units of MHz, of long-range  $2^\pm$  and  $3^\pm$  states in  ${}^3\text{He}(2\ {}^3\text{S}_1)+{}^3\text{He}(2\ {}^3\text{P}_j)$ . Energies given are relative to the energy of the specified asymptote. The superscripts 1 and 2 indicate those states which satisfy the strong coupling conditions  $\mathcal{A}_{\text{str}} > 0.9 E_h$  and  $\mathcal{A}_{\text{full}} > 0.9 E_h$  respectively.

Symmetry	State No.	Asympt. No.	$v/T$	0	1	2	3	4
$2^+$	6	3	0			1263.59	1167.37	1041.69
			1			483.739	400.323 <sup>2</sup>	292.599 <sup>2</sup>
			2			24.8937		
	7	4	0			1119.79 <sup>2</sup>	1013.79 <sup>2</sup>	875.239 <sup>2</sup>
			1			436.459 <sup>2</sup>	376.891 <sup>2</sup>	301.106 <sup>2</sup>
			2			143.028	105.268	58.7279 <sup>2</sup>
			3			10.5484		
	8	4	0			524.832 <sup>2</sup>	441.585 <sup>2</sup>	332.271 <sup>2</sup>
			1			932.947 <sup>2</sup>	853.811 <sup>1,2</sup>	749.864 <sup>1,2</sup>
			2			325.882 <sup>2</sup>	278.283 <sup>2</sup>	217.474 <sup>1,2</sup>
3					95.8030	71.0373	41.3769 <sup>1,2</sup>	
4					19.9633	10.0466		
5					87.8731 <sup>1,2</sup>	35.2247 <sup>1,2</sup>		
$2^-$	12	8	0			932.947 <sup>2</sup>	853.811 <sup>1,2</sup>	749.864 <sup>1,2</sup>
			1			325.882 <sup>2</sup>	278.283 <sup>2</sup>	217.474 <sup>1,2</sup>
			2			95.8030	71.0373	41.3769 <sup>1,2</sup>
			3			19.9633	10.0466	
	13	9	0			87.8731 <sup>1,2</sup>	35.2247 <sup>1,2</sup>	
			1			5.25868		
			2					
			3					
			4					
			5					
$3^+$	4	4	0				1623.55	1470.74
			1				568.235	468.826
			2				137.420	81.9036
			3				0.85611	
$3^-$	4	4	16				643.992 <sup>1,2</sup>	551.467 <sup>1,2</sup>
			17				150.116 <sup>1</sup>	97.8055
			18				1.20481	
			19					

sis of spin-conservation of the laser coupling that resonances which exist solely inside this distance will very likely ionize and hence will not be observed in experiment.

Beneath the lowest asymptote we find bound levels with only very weak coupling strengths. We therefore focus on the resonances that were successfully isolated. As these levels are not purely long-range, we must also consider the effect of ionization which reduces the level's lifetime and hence observability. In our previous investigation of  ${}^4\text{He}^*$  we imposed a criterion of  $P_{\text{str}} > 87.5\%$ . However, although a large number of resonances were found in  ${}^3\text{He}^*$  using the above method, very few satisfy the same observability criteria as  ${}^4\text{He}^*$ . In Table 3 we instead list the 30 resonances that are most likely to be observed in experiment, grouped by the nearest fine-structure asymptote.

In contrast to the purely long-range levels in the  $0_u^+$ ,  $J = 1$  potentials of  ${}^4\text{He}^*$ , we do not find any single-channel long-range bound levels in the  ${}^3\text{He}^*$  potentials that remain bound after the inclusion of couplings to all accessible states, nor do we find any multichannel levels that can be described purely in terms of single-channel potentials. Again we must emphasize that the relative coarseness of the approach here, necessitated by the large basis sets, may result in some important levels not being detected. Additionally, for the remaining resonances with short-range character, very few possess strong coupling strengths to the metastable manifold. We do note that there are

some particular resonances which stand out in that their short-range spin-stretch character is high with  $P_{\text{str}} > 80\%$ . It is these levels that we believe will be the most likely to be observed in experiment. We also note that the majority of resonances appear to be dominated both by  $T = 1$  and by a projection of  $\phi = 1$ .

## 4 Conclusions

The bound states of the fermionic  ${}^3\text{He}(2\ {}^3\text{S}_1)+{}^3\text{He}(2\ {}^3\text{P}_j)$  system, where  $j = 0, 1, 2$ , have been investigated using the recently available *ab initio* short-range  ${}^{1,3,5}\Sigma_{g,u}^+$  and  ${}^{1,3,5}\Pi_{g,u}$  potentials computed by Deguilhem *et al.* [8]. Single-channel and multichannel calculations have been undertaken in order to investigate the effects of Coriolis and non-adiabatic couplings. In contrast to the situation for the  ${}^4\text{He}^*$  system [9] where the effect of these couplings on the large number of bound levels below the lowest asymptote ( $j = 2$ ) could be studied, most of the levels for the  ${}^3\text{He}^*$  lie above the lowest asymptote and become resonances due to couplings to open channels.

The single-channel long-range levels obtained in the present investigation differ significantly from those found by Dickinson [11], both in their patterns and energies. Dickinson reports nine levels for the  $0^+$  symmetry, 16 for  $0^-$ , six for  $3^+$  and four for  $3^-$  whereas we find 22 levels for  $0^+$ , 35 for  $0^-$ , seven for  $3^+$  and five for  $3^-$ . We also find numerous levels for the  $1^\pm$

**Table 3** Energies, in units of MHz, of resonances in  ${}^3\text{He}(2\ {}^3\text{S}_1)+{}^3\text{He}(2\ {}^3\text{P}_j)$  that are most likely to be observable in experiment. Energies given are relative to the specified asymptotic energy  $E_N^\infty$ . The predissociation width  $\Gamma_{\text{pre}}$ , short-range spin-stretched character  $P_{\text{str}}$ , coupling strength  $\mathcal{A}_{\text{str}}$  and largest contributing basis of  $\phi$  are listed for each level.

$T$	$P_T$	$E$ (MHz)	$\Gamma_{\text{pre}}$ (MHz)	$P_{\text{str}}$ (%)	$\mathcal{A}_{\text{str}}(E_h)$	$\phi$
$E_2^\infty = 1780.85$ MHz						
2	-1	-1283.40	15.32	49.6	0.372	0
1	-1	-705.27	71.56	82.0	0.177	1
1	-1	-301.47	33.13	90.2	0.267	1
2	-1	-110.16	19.02	44.5	0.375	0
1	-1	-71.68	5.15	64.4	0.280	1
$E_3^\infty = 6292.91$ MHz						
2	-1	-1951.86	69.9	47.3	0.278	0
1	-1	-1808.40	60.4	49.1	0.313	1
1	-1	-1179.49	59.8	51.8	0.259	1
1	-1	-958.79	60.9	76.1	0.234	1
1	-1	-848.05	46.9	70.8	0.234	1
1	-1	-812.01	44.2	62.2	0.268	1
1	-1	-779.20	44.9	76.9	0.320	1
1	-1	-601.37	55.7	49.1	0.285	1
2	-1	-499.02	86.6	58.0	0.337	0
1	-1	-324.32	54.4	68.1	0.281	1
1	-1	-313.77	58.0	75.2	0.312	1
$E_4^\infty = 6739.70$ MHz						
2	-1	-193.32	58.1	51.3	0.301	1
2	-1	-186.29	36.0	55.1	0.372	1
1	-1	-38.44	64.7	59.7	0.290	1
1	-1	-11.52	76.6	58.0	0.269	1
$E_6^\infty = 8520.55$ MHz						
1	-1	-1029.50	20.1	76.5	0.204	1
1	-1	-840.44	24.9	83.8	0.212	1
1	-1	-513.78	42.3	84.8	0.204	1
1	-1	-380.48	53.7	84.0	0.190	1
1	-1	-245.71	55.3	73.0	0.213	1
$E_7^\infty = 13032.61$ MHz						
1	-1	-1996.78	91.1	76.6	0.157	0
1	-1	-680.18	86.2	80.5	0.182	1
1	-1	-552.73	76.3	74.2	0.172	1
1	-1	-508.69	92.0	76.1	0.190	1

and  $2^\pm$  symmetries for which Dickinson could not find any states. These differences are not unexpected as our expression (29) for the matrix elements of  $\hat{H}_{el}$  differs from that of Dickinson by an overall phase factor and the phase of the  $\Lambda_g - \Lambda_u$  term. By using the expressions given by Dickinson and with some modification of the values for hyperfine structure, our single-channel calculations were able to reproduce the results of Dickinson to within 5%.

The possible experimental observability of the theoretical levels has been assessed using criteria based upon the short-range character of each level and their coupling to metastable ground states. Although the bound states below the lowest asymptote and most of the large number of resonances above this asymptote do not satisfy our observability criteria we are able to identify some 30 resonances which are promising candidates to be observed in experiment. Unfortunately, the levels that were found in the single-channel calculations were not able to be linked to any of the predicted multichannel resonances. This is because we only have information regarding resonances that have small predissociation rates, instead of for the complete set of states. Hence it is very difficult to observe the change of behaviour of a single-channel bound level after the non-adiabatic and Coriolis terms are included. In contrast, the  $^4\text{He}^*$  calculation focused on multichannel bound levels which allowed a comparison between the complete set of single-channel and multichannel levels. For the short-range levels, this lack of connection implies that the non-adiabatic and Coriolis couplings modify the character of the levels such that they are no longer observable in experiment. However, because the resonance search is costly to perform, we cannot make the same statement for the purely long-range single-channel levels. Hence, we also recommend that future experiments also search for the levels that are marked in Tables 1 and 2 as observable.

## Appendix: Basis states and matrix elements

The unsymmetrized body-fixed (molecular) states in the coupling scheme (11) are

$$\begin{aligned} & |(\gamma_1 j_1 i_1 f_1)_A, (\gamma_2 j_2 i_2 f_2)_B, f, \Omega_f, T, m_T\rangle = \\ & |T, m_T, \Omega_f\rangle \sum_{\Omega_{f_1} \Omega_{f_2}} \sum_{\Omega_{j_1} \Omega_{j_2}} \sum_{\Omega_{i_1} \Omega_{i_2}} \sum_{\Omega_{L_1} \Omega_{L_2}} \sum_{\Omega_{S_1} \Omega_{S_2}} \\ & \times C_{\Omega_{f_1} \Omega_{f_2} \Omega_f}^{f_1 f_2 f} C_{\Omega_{j_1} \Omega_{j_2} \Omega_f}^{j_1 i_1 f_1} C_{\Omega_{i_2} \Omega_{i_2} \Omega_{f_2}}^{j_2 i_2 f_2} C_{\Omega_{L_1} \Omega_{S_1} \Omega_{j_1}}^{L_1 S_1 j_1} \\ & \times C_{\Omega_{L_2} \Omega_{S_2} \Omega_{j_2}}^{L_2 S_2 j_2} |\gamma_1 \Omega_{L_1} \Omega_{S_1}\rangle_A |i_1 \Omega_{i_1}\rangle_A \\ & \times |\gamma_2 \Omega_{L_2} \Omega_{S_2}\rangle_B |i_2 \Omega_{i_2}\rangle_B \end{aligned} \quad (50)$$

where the transformation between the molecular and space-fixed states is, for example,

$$|j \Omega_j\rangle = \sum_{m_j} D_{m_j \Omega_j}^j(\varphi, \theta, 0) |j m_j\rangle. \quad (51)$$

The states of the dimer system must be constructed to correctly include the symmetries present in the system. Importantly, they must be eigenstates of the total parity and nuclear permutation. The total parity operator  $\hat{P}_T$  is equivalent to the action of  $\hat{P}_L \hat{P}_S \hat{P}_i \hat{X}_N$  where the action of the inversion operators  $\hat{P}_L, \hat{P}_S$  and  $\hat{P}_i$  on the orbital, electronic spin and nuclear spin space-fixed states respectively is

$$\begin{aligned} \hat{P}_L |L_i m_{L_i}\rangle_A &= P_i |L_i m_{L_i}\rangle_B, \\ \hat{P}_S |S_i m_{S_i}\rangle_A &= |S_i m_{S_i}\rangle_B, \\ \hat{P}_i |i_i m_{i_i}\rangle_A &= |i_i m_{i_i}\rangle_B \end{aligned} \quad (52)$$

where  $P_i$  is the parity of the atomic state. The nuclear permutation operator  $\hat{X}_N$  reverses the molecular axis which is equivalent to  $A \leftrightarrow B$  and  $(\theta, \varphi) \rightarrow (\pi - \theta, \varphi + \pi)$ . Noting that

$$\begin{aligned} \hat{X}_N D_{m_j \Omega_j}^j(\varphi, \theta, 0) &= D_{m_j \Omega_j}^j(\varphi + \pi, \pi - \theta, 0) \\ &= (-1)^j D_{m_j, -\Omega_j}^j(\varphi, \theta, 0) \end{aligned} \quad (53)$$

then

$$\hat{P}_T |T, m_T, \Omega_f\rangle = (-1)^T |T, m_T, -\Omega_f\rangle \quad (54)$$

and

$$\begin{aligned} \hat{P}_T |(\alpha_1)_A, (\alpha_2)_B, f, \Omega_f, T, m_T\rangle = \\ P_1 P_2 (-1)^{f-T} |(\alpha_1)_A, (\alpha_2)_B, f, -\Omega_f, T, m_T\rangle \end{aligned} \quad (55)$$

where we have introduced the notation  $\alpha_i = \{j_i, i_i, f_i\}$ . The eigenstates of  $\hat{P}_T$  are therefore given by (14).

Since  $\hat{X}_N$  is equivalent to  $\hat{P}_T \hat{P}_L \hat{P}_S \hat{P}_i$  where

$$\begin{aligned} \hat{P}_L \hat{P}_S \hat{P}_i |(\alpha_1)_A, (\alpha_2)_B, f, \Omega_f, T, m_T\rangle = \\ (-1)^{f_1+f_2-f} P_1 P_2 |(\alpha_2)_A, (\alpha_1)_B, f, \Omega_f, T, m_T\rangle \end{aligned} \quad (56)$$

then the action of  $\hat{X}_N$  on the states (14) is

$$\begin{aligned} \hat{X}_N |(\alpha_1)_A, (\alpha_2)_B, f, \phi, T, m_T; P_T\rangle = \\ P_T P_1 P_2 (-1)^{f_1+f_2-f+N_1 N_2} \\ \times |(\alpha_2)_A, (\alpha_1)_B, f, \phi, T, m_T; P_T\rangle \end{aligned} \quad (57)$$

so that the eigenstates of  $\hat{X}_N$  are (15).

The relationship (21) between the bases (17) and (19) is obtained by first using

$$\begin{aligned} |\gamma_1 \Omega_{L_1} \Omega_{S_1}\rangle_A |\gamma_2 \Omega_{L_2} \Omega_{S_2}\rangle_B = \\ \sum_{LS \Omega_L \Omega_S} C_{\Omega_{L_1} \Omega_{L_2} \Omega_L}^{L_1 L_2 L} C_{\Omega_{S_1} \Omega_{S_2} \Omega_S}^{S_1 S_2 S} \\ \times |(\gamma_1)_A (\gamma_2)_B, LS \Omega_L \Omega_S\rangle, \end{aligned} \quad (58)$$

and expressing sums over Clebsch-Gordan coefficients as  $9 - j$  symbols to give

$$|(\alpha_1)_A, (\alpha_2)_B, f, \phi, T, m_T; P_T\rangle =$$

$$\begin{aligned}
|T, m_T, \phi\rangle & \sum_{\Omega_i} \sum_{\Omega_{i_2}} \sum_{ij\Omega_i\Omega_j LS\Omega_L\Omega_S} \\
& \times [ijLSj_1j_2f_1f_2]^{1/2} C_{\Omega_j\Omega_i\phi}^{jif} C_{\Omega_{i_1}\Omega_{i_2}\Omega_i}^{i_1i_2i} \\
& \times C_{\Omega_L\Omega_S\Omega_j}^{LSj} \begin{Bmatrix} j_1 & j_2 & j \\ i_1 & i_2 & i \\ f_1 & f_2 & f \end{Bmatrix} \begin{Bmatrix} L_1 & L_2 & L \\ S_1 & S_2 & S \\ j_1 & j_2 & j \end{Bmatrix} \\
& \times |(\gamma_1)_A(\gamma_2)_B, LS\Omega_L\Omega_S\rangle |i_1\Omega_{i_1}\rangle_A |i_2\Omega_{i_2}\rangle_B. \quad (59)
\end{aligned}$$

$$\begin{aligned}
& \times \begin{Bmatrix} 1 & j'_2 & j' \\ 1/2 & 1/2 & i' \\ f'_1 & f'_2 & f' \end{Bmatrix} \begin{Bmatrix} 1 & j_2 & j \\ 1/2 & 1/2 & i \\ f_1 & f_2 & f \end{Bmatrix} \\
& \times \begin{Bmatrix} 1 & 1 & j'_2 \\ 1 & j' & S' \end{Bmatrix} \begin{Bmatrix} 1 & 1 & j_2 \\ 1 & j & S \end{Bmatrix} \\
& \times \frac{1}{4} [(c_{iT}^{g'}\langle g'| + c_{iT}^{u'}\langle u'|)\hat{H}_{el}|c_{iT}^g|g\rangle + c_{iT}^u|u\rangle] \\
& \times \langle (i'_1)_A, (i'_1)_B, i', \Omega'_i | (i_1)_A, (i_1)_B, i, \Omega_i \rangle \quad (65)
\end{aligned}$$

Introducing the coupling coefficients, for example,

$$\begin{aligned}
F_{LS\Omega_L\Omega_S}^{j_1j_2j\Omega_j} & = [(2L+1)(2S+1)(2j_1+1)(2j_2+1)]^{\frac{1}{2}} \\
& \times C_{\Omega_L\Omega_S\Omega_j}^{LSj} \begin{Bmatrix} L_1 & L_2 & L \\ S_1 & S_2 & S \\ j_1 & j_2 & j \end{Bmatrix} \quad (60)
\end{aligned}$$

and using, from (19),

$$|(\gamma_1)_A(\gamma_2)_B, LS\Omega_L\Omega_S\rangle = N_w(|g\rangle + |u\rangle) \quad (61)$$

then

$$\begin{aligned}
|(\alpha_1)_A, (\alpha_2)_B, f, \phi, T, m_T; P_T\rangle & = \\
|T, m_T, \phi\rangle & \sum_{\Omega_i} \sum_{\Omega_{i_2}} \sum_{ij\Omega_i\Omega_j LS\Omega_L\Omega_S} C_{\Omega_{i_1}\Omega_{i_2}\Omega_i}^{i_1i_2i} \\
& \times F_{ji\Omega_j\Omega_i}^{f_1f_2f\phi} F_{LS\Omega_L\Omega_S}^{j_1j_2j\Omega_j} (|g\rangle + |u\rangle) |i_1\Omega_{i_1}\rangle_A |i_2\Omega_{i_2}\rangle_B. \quad (62)
\end{aligned}$$

The state with  $A \leftrightarrow B$  is obtained by reordering the angular momenta subscripted with 1 and 2 in all Clebsch-Gordan and  $9-j$  symbols and using

$$|(\gamma_2)_A(\gamma_1)_B, LS\Omega_L\Omega_S\rangle = N_w P_1 P_2 (-1)^{L_1+L_2-L+S_1+S_2-S} (|g\rangle - |u\rangle) \quad (63)$$

to give

$$\begin{aligned}
|(\alpha_2)_A, (\alpha_1)_B, f, \phi, T, m_T; P_T\rangle & = \\
|T, m_T, \phi\rangle & \sum_{\Omega_i} \sum_{\Omega_{i_2}} \sum_{ij\Omega_i\Omega_j LS\Omega_L\Omega_S} (-1)^{f_1+f_2+f+2i} \\
& \times C_{\Omega_{i_1}\Omega_{i_2}\Omega_i}^{i_1i_2i} F_{ji\Omega_j\Omega_i}^{f_1f_2f\phi} F_{LS\Omega_L\Omega_S}^{j_1j_2j\Omega_j} \\
& \times (|g\rangle - |u\rangle) |i_2\Omega_{i_2}\rangle_A |i_1\Omega_{i_1}\rangle_B. \quad (64)
\end{aligned}$$

Forming the combination (16) then yields (21).

The matrix elements of  $\hat{H}_{el}$  are diagonal in  $\phi$ . Using the explicit states (25) then

$$\begin{aligned}
\langle \alpha'_1, \alpha'_2, \phi' | \hat{H}_{el} | \alpha_1, \alpha_2, \phi \rangle & = \\
\langle T', m'_T, \phi' | T, m_T, \phi \rangle & \sum_{i'} \sum_{j'} \sum_{ij\Omega_i\Omega_j S'\Omega'_L\Omega'_S} \sum_{SS\Omega_S\Omega_S} (-1)^{j'_2+j_2} \\
& \times [i'j'f'_1f'_2S'j'_2ijf_1f_2Sj_2]^{1/2} \\
& \times C_{\Omega'_j\Omega'_i\phi'}^{j'if'} C_{\Omega_j\Omega_i\phi}^{jif} C_{\Omega'_L\Omega'_S\Omega'_j}^{1S'j'} C_{\Omega_L\Omega_S\Omega_j}^{1Sj}
\end{aligned}$$

where  $c_{iT}^g = 1 + (-1)^i P_T$  and  $c_{iT}^u = 1 - (-1)^i P_T$ . The orthogonality of states reduces this to

$$\begin{aligned}
\langle \alpha'_1, \alpha'_2, \phi' | \hat{H}_{el} | \alpha_1, \alpha_2, \phi \rangle & = \\
\delta_{\eta, \eta'} & \sum_{j'} \sum_{ij\Omega_i\Omega_j S\Omega_L\Omega_S} (-1)^{j'_2+j_2} [j'f'_1f'_2j'_2j f_1f_2j_2]^{1/2} [Si] \\
& \times C_{\Omega'_j\Omega'_i\phi'}^{j'if'} C_{\Omega_j\Omega_i\phi}^{jif} C_{\Omega_L\Omega_S\Omega'_j}^{1S'j'} C_{\Omega_L\Omega_S\Omega_j}^{1Sj} \\
& \times \begin{Bmatrix} 1 & j'_2 & j' \\ 1/2 & 1/2 & i' \\ f'_1 & f'_2 & f' \end{Bmatrix} \begin{Bmatrix} 1 & j_2 & j \\ 1/2 & 1/2 & i \\ f_1 & f_2 & f \end{Bmatrix} \begin{Bmatrix} 1 & 1 & j'_2 \\ 1 & j' & S \end{Bmatrix} \\
& \times \begin{Bmatrix} 1 & 1 & j_2 \\ 1 & j & S \end{Bmatrix} \frac{1}{2} [c_{iT}^g ({}^{2S+1}\Lambda_g^+(R) + E_{\Lambda S}^\infty) \\
& + c_{iT}^u ({}^{2S+1}\Lambda_u^+ + E_{\Lambda S}^\infty)] \quad (66)
\end{aligned}$$

where  $\eta = \{\gamma_1, \gamma_2, \phi, T, m_T, P_T\}$ . Similarly we can show

$$\begin{aligned}
\langle \alpha'_1, \alpha'_2, -\phi' | \hat{H}_{el} | \alpha_1, \alpha_2, -\phi \rangle & = \\
(-1)^{f-f'} \langle \alpha'_1, \alpha'_2, \phi' | \hat{H}_{el} | \alpha_1, \alpha_2, \phi \rangle. \quad (67)
\end{aligned}$$

The phase factor  $(-1)^{f-f'}$  is cancelled by the factor arising from (18), thus ensuring the two contributions (66) and (67) interfere constructively. Conversion of the Clebsch-Gordan coefficients into  $3-j$  symbols finally yields (29).

## Acknowledgements

Our initial interest in this problem was stimulated by some very interesting and helpful discussions with the late Professor Alan Dickinson of Newcastle University. Therefore we would like to take this opportunity to dedicate this paper to his memory.

## References

- 1 N. Herschbach, P. J. J. Tol, W. Vassen, W. Hogervorst, G. Woestenenk, J. W. Thomsen, P. van der Straten and A. Niehaus, *Phys. Rev. Lett.*, 2000, **84**, 1874–7.
- 2 J. Kim, U. D. Rapol, S. Moal, J. Léonard, M. Walhout and M. Leduc, *Eur. Phys. J. D*, 2004, **31**, 227–37.
- 3 M. van Rijnbach, *Dynamical spectroscopy of transient He<sub>2</sub> molecules*, Ph.D thesis, University of Utrecht, 2004.

- 4 J. Léonard, M. Walhout, A. P. Mosk, T. Müller, M. Leduc and C. Cohen-Tannoudji, *Phys. Rev. Lett.*, 2003, **91**, 073203.
- 5 J. Léonard, A. P. Mosk, M. Walhout, P. van der Straten, M. Leduc and C. Cohen-Tannoudji, *Phys. Rev. A*, 2004, **69**, 032702.
- 6 V. Venturi, P. J. Leo, E. Tiesinga, C. J. Williams and I. B. Whittingham, *Phys. Rev. A*, 2003, **68**, 022706.
- 7 A. S. Dickinson, F. X. Gadéa and T. Leininger, *Europhys. Lett.*, 2005, **70**, 320–6.
- 8 B. Deguilhem, T. Leininger, F. X. Gadéa and A. S. Dickinson, *J. Phys. B: At. Mol. Opt. Phys.*, 2009, **42**, 015102.
- 9 D. Cocks, I. B. Whittingham and G. Peach, *J. Phys. B: Atom. Molec. Opt. Phys.*, 2010, **43**, 135102.
- 10 R. J. W. Stas, J. M. McNamara, W. Hogervorst and W. Vassen, *Phys. Rev. Lett.*, 2004, **93**, 053001.
- 11 A. S. Dickinson, *Eur. Phys. J. D*, 2006, **37**, 435–9.
- 12 E. A. Hinds, J. D. Prestage and F. M. J. Pichanick, *Phys. Rev.*, 1985, **32**, 2615–21.
- 13 Q. Wu and G. W. F. Drake, *J. Phys. B: Atom. Molec. Opt. Phys.*, 2007, **40**, 393–402.
- 14 P. Zhao, J. R. Lawall and F. M. Pipkin, *Phys. Rev. Lett.*, 1991, **66**, 592–5.
- 15 J.-Y. Zhang, Z.-C. Yan, D. Vrinceanu, J. F. Babb and H. R. Sadeghpour, *Phys. Rev. A*, 2006, **73**, 022710.
- 16 W. J. Meath, *J. Chem. Phys.*, 1968 **48**, 227–35.
- 17 B. R. Johnson, *J. Chem. Phys.*, 1978, **69**, 4678–88.
- 18 J. M. McNamara, T. Jelte, A. S. Tychkov, W. Hogervorst and W. Vassen, *Phys. Rev. Lett.*, 2006, **97**, 080404.